
Article:
Ohkitani, K. (2018) Study of the 3D Euler equations using Clebsch potentials: dual mechanisms for geometric depletion. Nonlinearity, 31 (2). ISSN: 0951-7715

https://doi.org/10.1088/1361-6544/aa96cc

Study of the 3D Euler equations using Clebsch potentials: dual mechanisms for geometric depletion

Koji Ohkitani

School of Mathematics and Statistics
The University of Sheffield
Hicks Building, Hounsfield Road Sheffield S3 7RH, U.K.

E-mail: K.Ohkitani@sheffield.ac.uk

Abstract. After surveying analyses of the 3D Euler equations using the Clebsch potentials scattered over the literature, we report some preliminary new results.

1. Assuming that flow fields are free from nulls of the impulse and the vorticity fields, we study how constraints imposed by the Clebsch potentials lead to a degenerate geometrical structure, typically in the form of depletion of nonlinearity. We consider a vorticity surface spanned by $\boldsymbol{\omega}$ and another material vector $\boldsymbol{W}$ such that $\boldsymbol{\gamma} = \boldsymbol{\omega} \times \boldsymbol{W}$, where $\boldsymbol{\gamma}$ is the impulse variable in geometric gauge. We identify *dual* mechanism for geometric depletion and show that at least of one them is acting if $\boldsymbol{W}$ does not develop a null. This suggests that formation of singularity in flows endowed with Clebsch potentials is less likely to happen than in more general flows. Some arguments are given towards exclusion of "type I" blowup. A mathematical challenge remains to rule out singularity formation for flows which have Clebsch potentials everywhere.

2. We exploit classical differential geometry kinematically to write down the Gauss-Weingarten equations for the vorticity surface of the Clebsch potential in terms of fluid dynamical variables, as are the first, second and third fundamental forms. In particular, we derive a constraint on the size of the Gaussian curvature near the point of a possible singularity. On the other hand, an application of the Gauss-Bonnet theorem reveals that the tangential curvature of the surface becomes large in the neighborhood of near-singularity.

3. Using spatially-periodic flows with highly-symmetry, i.e. initial conditions of the Taylor-Green vortex and the Kida-Pelz flow, we present explicit formulas of the Clebsch potentials with exceptional singular surfaces where the Clebsch potentials are undefined. This is done by connecting the known expressions with the solenoidal impulse variable (i.e. the incompressible velocity) using suitable canonical transforms. By a simple argument we show that they keep forming material separatrices under the time evolution of the 3D Euler equations. We argue on this basis that a singularity, if developed, will be associated with these exceptional material surfaces. The difficulty of having Clebsch potentials globally on all of space have been with us for a long time. The proposal rather seeks to turn the difficulty into an advantage by using their absence to identify and locate possible singularities.

Keywords: 3D Euler equations, Clebsch potentials, geometric depletion, blowup, differential geometry, curvatures

1. Introduction

The vortex stretching mechanism in inviscid fluids associated with the incompressible 3D Euler equations is not well understood. It poses serious difficulty in mathematical handling of regularity issues. A possible formation of singularity leaves room for an interesting physical interpretation in connection with the onset of turbulence. At the moment, it seems a satisfactory mathematical treatment of the general incompressible fluids seems very difficult. One way to alleviate the difficulty is to go for geometrically simple flows and to try characterising them in some detail.

It is well-known that the vorticity plays a key role in the dynamics of the 3D Euler equations [5]. In particular, the curvature of vortex lines play an important role in controlling the regularity of the 3D Euler equations, see e.g. [18, 23]. Perhaps, geometrically the simplest example of flows of non-zero vorticity is given by a class of flows endowed with Clebsch potentials. In this class of flows, the vortex line is represented by the intersections of two material surfaces, that is, the vortex line is integrable. We may then ask how this stringent condition of integrability affects and possibly constrains development of intense vortex stretching.

After reviewing known results on a class of flows with Clebsch potentials obtained by many authors so far, we study how the vortex stretching process in 3D Euler flows is constrained in this class of flows. In particular, we identify the dual mechanisms for geometric depletion and classify scenarios based on alignment properties. Under certain conditions we argue that it is unlikely for a type I blowup to develop.

Classical differential geometry of surfaces is exploited for the characterisation of the vorticity surface. We derive a constraint on the size of Gaussian curvature of the vorticity surface, while showing that the tangential curvature becomes large, if a singularity is to develop.

We present specific examples of Clebsch potentials, in particular, for the Taylor-Green and the Kida-Pelz flow. It is known that Clebsch potentials are unlikely to be available near nulls of the impulse [28] and unavailable near generic vorticity nulls [35]. Examples given here clarify that Clebsch potentials can have singularities at points which are not even nulls of the impulse or the vorticity. Combining this recognition with the above result, we propose to use the exceptional set of points to identify candidates of (near-)singularities.

The rest of the paper is organised as follows. In Section 2, we survey known results regarding Clebsch potentials. In Section 3, kinematics of Clebsch potentials is developed and used to reveal two mechanisms of nonlinearity depletion. In Section 4, we derive a set of equations for the vorticity surface and study its curvatures on the basis of classical differential geometry. Finally, Section 5 is devoted to summary and outlook.

2. Basics elements of Clebsch potentials

We consider the incompressible 3D Euler equations with standard notations

$$\frac{D\boldsymbol{u}}{Dt} = -\nabla p, \tag{1}$$
$$\nabla \cdot \boldsymbol{u} = 0,$$

or equivalently the vorticity equations

$$\frac{D\boldsymbol{\omega}}{Dt} = (\boldsymbol{\omega} \cdot \nabla)\boldsymbol{u}, \tag{2}$$

where $\boldsymbol{u}, p$ and $\boldsymbol{\omega}$ denote the velocity, the pressure and the vorticity.

Yet another formulation of incompressible fluids is given by the impulse variable, see e.g. [61]. In geometric gauge, it satisfies

$$\frac{D\boldsymbol{\gamma}}{Dt} = -\boldsymbol{\gamma} \cdot (\nabla \boldsymbol{u})^T, \tag{3}$$

where T denotes matrix transpose. It is noted that equations (1), (2) and (3) are all equivalent.

2.1. Fundamentals

In this and subsequent subsections, we summarise known facts about Clebsch potentials. When we can write

$$\boldsymbol{u} = f\nabla g - \nabla \phi \tag{4}$$

in a domain under consideration, we say that the flow has Clebsch potentials f and g ‡ [16, 17]. This is possible at least locally, see [2, 64] or **Appendix A**. If Clebsch potentials are available, we can take the impulse variable $\boldsymbol{\gamma}$ as

$$\boldsymbol{\gamma} = f\nabla g. \tag{5}$$

The vector field of this form was introduced and called "complex-lamellar" in connection with the problem of magnetism [71]. See also [57, 31, 74].

It is possible to have (4) locally, but to have them in a domain, the Frobenius condition of integrability should be satisfied. For a lucid exposition of the integrability condition, see an appendix of [10]. Actually, care should be taken if nulls of the impulse or the vorticity are present in the flow (see Subsection 2.3 below). In terms of $\boldsymbol{\gamma}$, the Frobenius condition is given by vanishing of 'helicity' of $\boldsymbol{\gamma}$ in the flow [28]

$$\boldsymbol{\gamma} \cdot \nabla \times \boldsymbol{\gamma} = 0. \tag{6}$$

‡ The potentials $f, g, -\phi$ are also called Monge potentials. Clebsch potentials are sometimes referred to under the names of Euler, Darboux and Pfaff. [73]

See also [41] for an application of zero-helicity flows. The condition (6) is necessary, but (only) nearly sufficient for (5) to hold. In other words,

$$\boldsymbol{\gamma} = f\nabla g \Longrightarrow \boldsymbol{\gamma} \cdot \nabla \times \boldsymbol{\gamma} = 0$$

holds true everywhere, but its converse

$$\boldsymbol{\gamma} = f\nabla g \Longleftarrow \boldsymbol{\gamma} \cdot \nabla \times \boldsymbol{\gamma} = 0$$

does not hold everywhere. Actually, there is an exceptional set of points, which is 'thin,' i.e. of measure zero in all the examples considered in this paper. Nulls of $\boldsymbol{\gamma}$ or $\boldsymbol{\omega}$ are the candidates for such an exceptional set of points. It is expected that the converse holds almost everywhere, but the author is unaware of its proof.

It is well known that

$$\frac{D}{Dt}(\boldsymbol{\gamma} \cdot \nabla \times \boldsymbol{\gamma}) = 0,$$

hence the zero-helicity condition of $\boldsymbol{\gamma}$ persists under time evolution if it is so initially.

The vorticity can be written

$$\boldsymbol{\omega} = \nabla \times (f\nabla g) = \nabla f \times \nabla g, \tag{7}$$

and the helicity density

$$\boldsymbol{u} \cdot \boldsymbol{\omega} = -\boldsymbol{\omega} \cdot \nabla\phi = -\frac{\partial \phi}{\partial u},$$

where u is the arc-length parameter along the vortex line. It follows that

$$\phi = -\int \boldsymbol{u} \cdot \boldsymbol{\omega} du = -\int \frac{\boldsymbol{u} \cdot \boldsymbol{\omega}}{\boldsymbol{\omega} \cdot \nabla\theta} d\theta,$$

where $\theta = F(u)$ is a parameter such that $\frac{d\boldsymbol{x}}{du} = \boldsymbol{\omega}(\boldsymbol{x}(u))$, [16].

We recall that the choice of f, g are far from being unique, as they are determined only up to canonical transformations, e.g. [43, 44, 25, 69]. More precisely, any pair of functions F, G which satisfies

$$\frac{\partial(F, G)}{\partial(f, g)} = 1$$

can equally play the same role. In fact, we can equivalently write

$$\boldsymbol{u} = F\nabla G - \nabla\Phi,$$

where

$$f = \frac{\partial S}{\partial g},\ F = -\frac{\partial S}{\partial G} \text{ with } \Phi = \phi - S(g, G).$$

Here $S(g, G)$ is an arbitrary generating function associated with gauge freedom.

Finally, consider the contraposition $f \leftrightarrow g$ in (7), which corresponds to $\boldsymbol{\omega} \to -\boldsymbol{\omega}$. By time-reversal, the Euler equations remain invariant under these changes.

The references on Clebsch potentials seem to be scattered over a range of literature. Older references include [38, 24, 1, 4, 36, 66, 72, 60]. More recent ones are [6, 40, 47, 76, 27, 62, 14, 42, 45, 54, 21, 75, 33]. Clebsch potentials appear in a variational formulation of fluid dynamics. See e.g. [22, 9, 48, 65, 46, 63, 7] in this context.

2.2. Truesdell's formula

If $\boldsymbol{\omega}(\boldsymbol{x},t)$ and one of the Clebsch potentials, say $g(\boldsymbol{x},t)$, are given, it is possible to construct the other one in a sufficiently small neighborhood as

$$f = \int_C \frac{\boldsymbol{c}\times\boldsymbol{\omega}\cdot d\boldsymbol{x}}{\boldsymbol{c}\cdot\nabla g},$$

where C is a path lying entirely on the surface $g=$ const and $\boldsymbol{c}$ is a constant vector such that $\boldsymbol{c}\cdot\nabla g\neq 0$ [73, 72]. (A minus sign in [73] should be removed.)

The derivation is straightforward, but is reproduced here for completeness. We compute that

$$\boldsymbol{\omega}\times\boldsymbol{c} = (\nabla f\times\nabla g)\times\boldsymbol{c} = (\boldsymbol{c}\cdot\nabla f)\nabla g - (\boldsymbol{c}\cdot\nabla g)\nabla f,$$

and because $d\boldsymbol{x}$ lies on a surface $g=$ const,

$$d\boldsymbol{x}\cdot(\boldsymbol{\omega}\times\boldsymbol{c}) = -(\boldsymbol{c}\cdot\nabla g)\,d\boldsymbol{x}\cdot\nabla f = -(\boldsymbol{c}\cdot\nabla g)df.$$

When g is given by a material surface $g(\boldsymbol{x},t) = G(\boldsymbol{a}(\boldsymbol{x},t))$, we can construct a corresponding function F by

$$F = \int_{C'} \frac{\widetilde{\boldsymbol{c}}\times\boldsymbol{\omega}(0)\cdot d\boldsymbol{a}}{\widetilde{\boldsymbol{c}}\cdot\nabla_{\boldsymbol{a}}G}.$$

We have the identity

$$\frac{\boldsymbol{c}\times\boldsymbol{\omega}\cdot d\boldsymbol{x}}{\boldsymbol{c}\cdot\nabla g} = \frac{(\boldsymbol{c}\cdot\nabla\boldsymbol{a})\times\boldsymbol{\omega}(0)\cdot d\boldsymbol{a}}{(\boldsymbol{c}\cdot\nabla\boldsymbol{a})\cdot\nabla_{\boldsymbol{a}}G},$$

whose numerator follows from the definition of Jacobian determinant and Cauchy formula. By taking $\widetilde{\boldsymbol{c}} = \boldsymbol{c}\cdot\nabla\boldsymbol{a}$, we find $f(\boldsymbol{x},t) = F(\boldsymbol{a}(\boldsymbol{x},t))$, which shows that f is also material.

2.3. No-go theorems

It is known when a null (that is, a zero) of the impulse variables is present, we do not expect that Clebsch potentials are available in that neighborhood. An elementary counter-example is reproduced here from p.96 of [28], after converting the differential form notations to our current vectorial ones. We recall that if $\boldsymbol{\gamma} = f\nabla g$ with $|\boldsymbol{\gamma}|\neq 0$, $\nabla\times\boldsymbol{\gamma} = \nabla f\times\nabla g = \nabla f\times(f^{-1}\boldsymbol{\gamma}) = \boldsymbol{\theta}\times\boldsymbol{\gamma}$, where $\boldsymbol{\theta}\equiv\nabla\ln|f|$, because $f\neq 0$. Clearly, $\boldsymbol{\gamma}\cdot(\nabla\times\boldsymbol{\gamma}) = 0$.

Consider $\boldsymbol{\gamma} = (-y,x,0)^T$, which has a zero at the origin. The corresponding form $\gamma_1 dx + \gamma_2 dy = 0$ has integral curves $ax+by=0$, with constants a,b. It is, however, impossible to choose $\boldsymbol{\theta}$ in such a way that $\nabla\times\boldsymbol{\gamma} = \boldsymbol{\theta}\times\boldsymbol{\gamma}$. To see this, note $\nabla\times\boldsymbol{\gamma} = (0,0,2)^T$ on one hand. We compute on the other hand that $\boldsymbol{\theta}\times\boldsymbol{\gamma} = (0,0,Ax+By)$ for $\boldsymbol{\theta} = (A,B,0)^T$. Hence we deduce $Ax+By=2$, which fails at the origin. This is an example where Clebsch potentials are unavailable in the neighborhood of a null of $\boldsymbol{\gamma}$ even in two dimensions.

It is also known that Clebsch potentials do not exist near *generic* null points of $\boldsymbol{\omega}$, where generic means 'structurally stable', that is, persistence under small perturbations [35]. More precisely, by writing

$$\boldsymbol{\omega} = \boldsymbol{M}\boldsymbol{r} + O(r^2)$$

they have shown two things:
(1) If there are Clebsch potentials at a point, then $\det(\boldsymbol{M}) = 0$,
(2) The vorticity generically vanishes at a point if and only if $\det(\boldsymbol{M}) \neq 0$ there.
Combining these, they have proved Clebsch potentials do not exist near generic nulls of vorticity. See also [34].

These facts are often interpreted as obstacles in utilising Clebsch potentials in fluid mechanics. Here we will take an alternative view showing how we may possibly take advantage of the absence of Clebsch potentials, by finding out the implications that it entails.

3. Kinematics of Clebsch potentials

3.1. Preliminaries

We consider a point in space where $\boldsymbol{\gamma}$ and $\boldsymbol{\omega} \neq 0$. Given that

$$\boldsymbol{\gamma} \cdot \boldsymbol{\omega} \equiv 0,$$

we can choose a vector $\boldsymbol{W}$ such that

$$\boldsymbol{\gamma} = \boldsymbol{\omega} \times \boldsymbol{W} \tag{8}$$

holds. Because $\boldsymbol{\gamma}$ represents a normal vector to a material surface (an infinitesimal area element), $\boldsymbol{W}$ can be taken as a material vector (an infinitesimal line element) just as $\boldsymbol{\omega}$. Note that $\boldsymbol{W}$ is a passive vector, whose evolution is affected by the velocity, but which does not affect that of the velocity. In contrast, $\boldsymbol{\omega}$ and $\boldsymbol{\gamma}$ are active vectors, because they affect the evolution of velocity, e.g. through the Biot-Savart relationship.

Now consider a vorticity surface which is given by $g = $ const. specified by two parameters u and v (Figure 1). Let us parametrise $\boldsymbol{\omega}$ and $\boldsymbol{W}$ on the vorticity surface as

$$\frac{\partial \boldsymbol{x}}{\partial u} = \boldsymbol{\omega}(\boldsymbol{x}(u,v),t), \frac{\partial \boldsymbol{x}}{\partial v} = \boldsymbol{W}(\boldsymbol{x}(u,v),t), \tag{9}$$

where a pair of parameters (u, v) represents the vorticity surface in question. Note that $\frac{\partial}{\partial u} = \boldsymbol{\omega} \cdot \nabla$ and $\frac{\partial}{\partial v} = \boldsymbol{W} \cdot \nabla$.

The vector $\boldsymbol{W}$ satisfies the equations for a passive vector defined by

$$\frac{D\boldsymbol{W}}{Dt} = (\boldsymbol{W} \cdot \nabla)\boldsymbol{u}, \tag{10}$$

or

$$\frac{\partial \boldsymbol{W}}{\partial t} = (\boldsymbol{W} \cdot \nabla)\boldsymbol{u} - (\boldsymbol{u} \cdot \nabla)\boldsymbol{W}$$

$$= \nabla \times (\boldsymbol{u} \times \boldsymbol{W}) - \boldsymbol{u}(\nabla \cdot \boldsymbol{W}),$$

where use has been made of an identity

$$\nabla \times (\boldsymbol{u} \times \boldsymbol{W}) = (\boldsymbol{W} \cdot \nabla)\boldsymbol{u} - (\boldsymbol{u} \cdot \nabla)\boldsymbol{W} + \boldsymbol{u}(\nabla \cdot \boldsymbol{W}) - \boldsymbol{W}(\nabla \cdot \boldsymbol{u}).$$

It follows that

$$\frac{\partial}{\partial t}(\nabla \cdot \boldsymbol{W}) + \boldsymbol{u} \cdot \nabla(\nabla \cdot \boldsymbol{W}) = 0,$$

that is,

$$\frac{D}{Dt}\nabla \cdot \boldsymbol{W} = 0.$$

Hence we have $\nabla \cdot \boldsymbol{W} = C(\boldsymbol{a})$ independent of time, where $\boldsymbol{a}$ is a Lagrangian marker variable.

We check consistency of the above argument with $\boldsymbol{\omega} = \nabla \times \boldsymbol{\gamma}$ by computing that

$$\begin{aligned}
\boldsymbol{\omega} &= \nabla \times (\boldsymbol{\omega} \times \boldsymbol{W}) \\
&= (\boldsymbol{W} \cdot \nabla)\boldsymbol{\omega} - (\boldsymbol{\omega} \cdot \nabla)\boldsymbol{W} + \boldsymbol{\omega}(\nabla \cdot \boldsymbol{W}) - \boldsymbol{W}(\nabla \cdot \boldsymbol{\omega}) \\
&= \frac{\partial \boldsymbol{\omega}}{\partial v} - \frac{\partial \boldsymbol{W}}{\partial u} + \boldsymbol{\omega}(\nabla \cdot \boldsymbol{W}) \\
&= C(\boldsymbol{a})\boldsymbol{\omega}.
\end{aligned}$$

The first two terms cancel because of (9) on the vorticity surface and $\nabla \cdot \boldsymbol{\omega} = 0$. Therefore $C(\boldsymbol{a}) = 1$, or $\nabla \cdot \boldsymbol{W} = 1$. Thus $\boldsymbol{W}$ is not incompressible, unlike $\boldsymbol{\omega}$.

3.2. Alignment and stretching

Consider the spectrum $(\lambda_1, \lambda_2, \lambda_3)$ of the rate-of-strain tensor $\boldsymbol{S}$, corresponding to the eigenvectors $\boldsymbol{e}_1, \boldsymbol{e}_2, \boldsymbol{e}_3$, whose eigenvalues satisfy $\lambda_1 \geq \lambda_2 \geq \lambda_3$ and $\lambda_1 + \lambda_2 + \lambda_3 = 0$. There are two cases: $(+, +, -)$ where $\lambda_1, \lambda_2 \geq 0, \lambda_3 < 0$ and $(+, -, -)$ where $\lambda_1 \geq 0, \lambda_2, \lambda_3 < 0$.

We recall the stretching rates for $\boldsymbol{\omega}$ and $\boldsymbol{W}$ [56] are defined by

$$\alpha = \frac{D}{Dt}\log|\boldsymbol{\omega}| = \widehat{\boldsymbol{\omega}} \cdot \boldsymbol{S} \cdot \widehat{\boldsymbol{\omega}}, \quad \alpha_W = \frac{D}{Dt}\log|\boldsymbol{W}| = \widehat{\boldsymbol{W}} \cdot \boldsymbol{S} \cdot \widehat{\boldsymbol{W}},$$

where $\widehat{\ }$ denotes a unit vector, e.g. $\widehat{\boldsymbol{\omega}} = \boldsymbol{\omega}/|\boldsymbol{\omega}|$. We also define the similar rates for ∇f and ∇g by

$$\alpha_f = \frac{D}{Dt}\log|\nabla f| = -\widehat{\nabla f} \cdot \boldsymbol{S} \cdot \widehat{\nabla f}, \quad \alpha_g = \frac{D}{Dt}\log|\nabla g| = -\widehat{\nabla g} \cdot \boldsymbol{S} \cdot \widehat{\nabla g}.$$

Growth of $|\boldsymbol{\omega}|$ results from alignment with the eigenvector with a positive eigenvalue and that of $|\nabla f|, |\nabla g|$ results from alignment with the eigenvector with a negative eigenvalue. Also, shrinkage of $|\boldsymbol{W}|$ results from alignment with the eigenvector with a negative eigenvalue. For example, if $\boldsymbol{\omega}$ tends to align with $\boldsymbol{e}_2$, the intermediate eigenvector of $\boldsymbol{S}$, the we have $\alpha \to \lambda_2$.

For simplicity, we restrict our attention to the so-called type I blowup§ where singularity forms with marginal rates allowed by the Beale-Kato-Majda (hereafter, BKM) criterion [5].

3.3. Dual representations for geometric depletion

A mechanism of nonlinearity depletion was proposed in [54]. Schematically, it may be explained as follows. The first one is based on (7).

Representation 1

$$\underbrace{\boldsymbol{\omega}}_{O\left(\frac{1}{t_*-t}\right)} = \underbrace{\nabla f}_{O\left(\frac{1}{\sqrt{t_*-t}}\right)} \times \underbrace{\nabla g}_{O\left(\frac{1}{\sqrt{t_*-t}}\right)}$$

$$\text{line element} = \text{area element} \times \text{area element}$$

We recall that $\boldsymbol{\omega}$ satisfies the same equations for a line element, whereas ∇f and ∇g those for an area element [61]. In the above expression, the minimal rate of blow-up for the vorticity at $t = t_*$

$$\|\boldsymbol{\omega}\|_{L^\infty} = O\left(\frac{1}{t_*-t}\right)$$

is given by the BKM criterion [5], whereas those for scalar gradients ∇f and ∇g are

$$\|\nabla f\|_{L^\infty},\ \|\nabla g\|_{L^\infty} = O\left(\frac{1}{\sqrt{t_*-t}}\right)$$

given by [20].

It is clear that strength of singularity is balanced on both sides, provided that the two vectors are not parallel $\nabla f \nparallel \nabla g$. However, if ∇f and ∇g tend to align themselves sufficiently fast, the possibility of a marginal blow-up leads to a contradiction and hence can be ruled out. This is regarded as a possible mechanism of nonlinearity depletion. [54]

We introduce yet another mechanism of geometric degeneracy,based on (8), which is closely related to the above depletion.

Representation 2

$$\underbrace{\boldsymbol{\gamma}}_{O\left(\frac{1}{\sqrt{t_*-t}}\right)} = \underbrace{\boldsymbol{\omega}}_{O\left(\frac{1}{t_*-t}\right)} \times \underbrace{\boldsymbol{W}}_{O(\text{undetermined})}$$

$$\text{area element} = \text{line element} \times \text{line element}$$

This may be regarded as a dual to the above scheme in the sense that $\boldsymbol{\gamma}$ satisfies the same equations for an area element, whereas $\boldsymbol{\omega}$ and $\boldsymbol{W}$ those for a line element. Because

§ Strictly speaking, this is a slight abuse of terminology, because no differential inequality is available for $\|\boldsymbol{\omega}\|_{L^\infty}$, which is a critical norm.

$\boldsymbol{W}$ is a passive material vector, its minimal rate of blowup cannot be determined, unlike the BKM criterion for the vorticity. The symbol O(undetermined) in the above diagram stems from its passive nature.‖ We can only fix it, say, when it aligns with one of the eigenvectors of $\boldsymbol{S}$.

This alternative form of depletion is complementary to the Representation 1 above. There are two kinds of possible depletion; one is the case where ∇f becomes parallel to ∇g, and the other case where $\boldsymbol{\omega}$ becomes parallel to $\boldsymbol{W}$. We will see below how they are related to each other.

3.4. Analysis of dual mechanisms

By (7) we may derive a simple, but nevertheless useful identities as follows. We have

$$\boldsymbol{\gamma} = \boldsymbol{\omega} \times \boldsymbol{W} = (\nabla f \times \nabla g) \times \boldsymbol{W}$$

$$= (\boldsymbol{W} \cdot \nabla f)\nabla g - (\boldsymbol{W} \cdot \nabla g)\nabla f.$$

On the other hand, because of $\boldsymbol{\gamma} = f\nabla g$, we find

$$\boldsymbol{W} \cdot \nabla f = f, \tag{11}$$

$$\boldsymbol{W} \cdot \nabla g = 0, \tag{12}$$

provided that $\nabla f \nparallel \nabla g$ and $|\nabla f|, |\nabla g| \neq 0$. Note that (11) is consistent with the fact that f is material:

$$\frac{D}{Dt}\boldsymbol{W} \cdot \nabla f = \boldsymbol{W} \cdot \nabla \frac{D}{Dt} f = 0,$$

which is an alternative form of commutation of $\boldsymbol{W} \cdot \nabla$ and D/Dt, that is, $\left[\frac{D}{Dt}, \boldsymbol{W} \cdot \nabla\right] = 0$.

Let us denote the angle between ∇f and ∇g by θ_1 and the angle between $\boldsymbol{\omega}$ and $\boldsymbol{W}$ by θ_2, see Figure 1. We then have

$$|\sin\theta_1| = \frac{|\boldsymbol{\omega}|}{|\nabla f||\nabla g|} = \frac{|f||\boldsymbol{\omega}|}{|\nabla f||\boldsymbol{\gamma}|}$$

by (7) and

$$|\sin\theta_2| = \frac{|\boldsymbol{\gamma}|}{|\boldsymbol{\omega}||\boldsymbol{W}|}.$$

by (8). Looking at these expressions separately, we cannot tell how θ_1 or θ_2 behaves when $|\boldsymbol{\omega}|, |\boldsymbol{\gamma}|, |\boldsymbol{W}|$ and $|\nabla f|$ become large. However, it follows from their product that

$$|\sin\theta_1 \sin\theta_2| = \frac{|f|}{|\boldsymbol{W}||\nabla f|}. \tag{13}$$

‖ There is no way to show that e.g. the integral $\int_0^T \|\boldsymbol{W}\|_{L^\infty} dt$ bounds the Sobolev norms of the velocity because of lack of the Biot-Savart formula, which is available for $\boldsymbol{\omega}$.

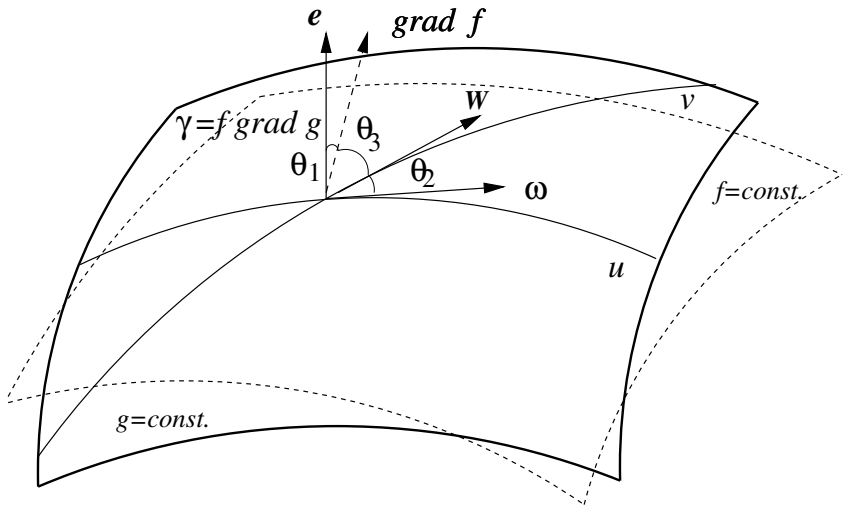

Figure 1. The vorticity surface g =constant, whose normal is $\boldsymbol{\gamma}$ is parameterised by (u, v).

Now let θ_3 be the angle between $\boldsymbol{W}$ and ∇f (Figure 1), we have by (11)

$$|f| = |\boldsymbol{W}||\nabla f||\cos\theta_3|, \tag{14}$$

and we thus conclude

$$|\sin\theta_1 \sin\theta_2| = |\cos\theta_3|. \tag{15}$$

The simple expressions (11, 12, 15) are the key results of this section. We will discuss their implications below.

3.5. Classification and heuristic exclusion of type I blowup

Type I singularity, which may be the simplest possible scenario of blowup, has not been excluded for the Euler equations. It has not been excluded for the Navier-Stokes equations, except for the axisymmetric case.

We are in a position to constrain type I blowup on the basis of (15). The main idea is to show that under this condition $|\nabla f| \to \infty$, if $|\boldsymbol{W}|$ does not develop a null, then $\theta_3 \to \pi/2$ by (11). Therefore under the condition we deduce by (15) that either $\theta_1 \to 0$ or $\theta_2 \to 0$. More detailed classifications will go as follows.

(i) The case $(+,+,-)$. We consider Representation 1, together with the alignment property and the minimal rates of blowup.

$$\begin{array}{ccccc} \boldsymbol{\omega} & = & \nabla f & \times & \nabla g \\ \boldsymbol{e}_{1 \text{ or } 2} & & \boldsymbol{e}_3 & & \boldsymbol{e}_3 \\ O\left(\frac{1}{t_*-t}\right) & & O\left(\frac{1}{\sqrt{t_*-t}}\right) & & O\left(\frac{1}{\sqrt{t_*-t}}\right) \end{array}$$

Assuming that ∇f tends to align with ∇g sufficiently fast, that is, the angle θ_1 between them approaching zero as $(t_* - t)^p$ for some $p > 0$, we can rule out this case. This can be done by contradiction because both sides are unbalanced.

(ii) The case $(+, -, -)$. If we accept the numerical result that the vorticity aligns with the intermediate rate-of-strain e.g. [3], this possibility can be discarded straight away. Otherwise we can still argue as follows.

(a) If $\boldsymbol{W}$ does not develop a null $|\boldsymbol{W}| \nrightarrow 0$, then we have $\theta_3 \to \pi/2$. There are two possibilities.

1. $\theta_1 \to 0$, that is, $\nabla f \parallel \nabla g$. We can rule this case out, if $\nabla f \parallel \nabla g$ sufficiently fast, as in (i).
2. $\theta_2 \to 0$, that is, $\boldsymbol{\omega} \parallel \boldsymbol{W}$. (See Subsection 3.7 on this possibility.) In this case Representation 2 look like as follows. This case is not completely

$$\begin{array}{ccccc} \boldsymbol{\gamma} & = & \boldsymbol{\omega} & \times & \boldsymbol{W} \\ \boldsymbol{e}_{2 \text{ or } 3} & & \boldsymbol{e}_1 & & \boldsymbol{e}_1 \\ O\left(\frac{1}{\sqrt{t_*-t}}\right) & & O\left(\frac{1}{t_*-t}\right) & & O\left(\frac{1}{t_*-t}\right) \end{array}$$

ruled out, but it is possible only under very special circumstances where the angle θ_2 is closing as $(t_* - t)^{3/2}$. However, this seems to be a slim possibility, as such a condition is too stringent.

(b) If $\boldsymbol{W}$ develops a null $|\boldsymbol{W}| \to 0$. In this case, the two Representations look as follows. Note that we have inevitably $\boldsymbol{W} \parallel \nabla f$ because γ and ∇g

$$\begin{array}{ccccccccccc} \boldsymbol{\gamma} & = & \boldsymbol{\omega} & \times & \boldsymbol{W} & & \boldsymbol{\omega} & = & \nabla f & \times & \nabla g \\ \boldsymbol{e}_{2 \text{ or } 3} & & \boldsymbol{e}_1 & & \boldsymbol{e}_{3 \text{ or } 2} & & \boldsymbol{e}_1 & & \boldsymbol{e}_{3 \text{ or } 2} & & \boldsymbol{e}_{2 \text{ or } 3} \\ O\left(\frac{1}{\sqrt{t_*-t}}\right) & & O\left(\frac{1}{t_*-t}\right) & & O\left(\sqrt{t_*-t}\right) & & O\left(\frac{1}{t_*-t}\right) & & O\left(\frac{1}{\sqrt{t_*-t}}\right) & & O\left(\frac{1}{\sqrt{t_*-t}}\right) \end{array}$$

are co-linear $\boldsymbol{\gamma} = f \nabla g$. We can rule out this configuration in the sense that it is not sustainable, i.e. inconsistent with the time evolution of the Euler equations. (See the next Subsection 3.6.) Overall, this semi-empirical arguments based on the alignment properties shows that type I blowup is less likely to happen in flows with Clebsch potentials than in more general flows. A mathematical challenge remains here to justify the heuristic arguments. Differential geometric approach in the next section is a possible option.

3.6. Non-persistence of the state of maximal helicity

This subsection explains the reason why the option (ii)(b) is excluded.

Consider a passive material vector $\boldsymbol{W}$ and an area element $\boldsymbol{A}$. We study whether the state of maximal helicity $\boldsymbol{W} \parallel \boldsymbol{A}$ persists under time evolution or not, on the basis of alignment of dependent variable vectors. We have generally

$$\frac{D}{Dt}\boldsymbol{W} \times \boldsymbol{A} = (\boldsymbol{V} \cdot \boldsymbol{W}) \times \boldsymbol{A} - \boldsymbol{W} \times (\boldsymbol{V}^T \cdot \boldsymbol{A}),$$

where T denotes a matrix transpose. Assuming $\boldsymbol{A} = c\boldsymbol{W}$ with a constant c, it can be readily checked using standard calculations e.g.[53, 52, 32] that

$$\frac{D}{Dt}\boldsymbol{W} \times \boldsymbol{A} = 2c(\boldsymbol{S} \cdot \boldsymbol{W}) \times \boldsymbol{W}.$$

This expression indeed vanishes when $\boldsymbol{S} \cdot \boldsymbol{W} = \lambda \boldsymbol{W}$ for some λ to the leading-order and the configuration is maintained. However, to the next-order it is easily verified that

$$\frac{D^2}{Dt^2}(\boldsymbol{W} \times \boldsymbol{A}) = -2c(\boldsymbol{P} \cdot \boldsymbol{W}) \times \boldsymbol{W} - 2c(\boldsymbol{\Omega} - \boldsymbol{S}) \cdot \boldsymbol{\Omega} \cdot \boldsymbol{W} \times \boldsymbol{W} + 2c(\boldsymbol{S} \cdot \boldsymbol{W}) \times \boldsymbol{V} \cdot \boldsymbol{W}, \quad (16)$$

where $\boldsymbol{\Omega} = \frac{1}{2}\left(\nabla \boldsymbol{u} - (\nabla \boldsymbol{u})^T\right)$ denotes the vorticity tensor and $\boldsymbol{P} = (\nabla \otimes \nabla)p$ the pressure Hessian. The right-hand side of (16) does not vanish in general, even if we assume that $\boldsymbol{S} \cdot \boldsymbol{W} = \lambda \boldsymbol{W}$. This means that this configuration does not persist under the time evolution of the 3D Euler equations.

3.7. A perfect alignment of two material vectors implies blowup

This is an additional remark on the alignment. It seems to be trivial, but apparently its proof has not been given before. It can be proven by contradiction.

Consider two material vectors $\boldsymbol{\omega}$ and $\boldsymbol{W}$ subject to a flow governed by the Euler equations:

$$\frac{D\boldsymbol{\omega}}{Dt} = (\boldsymbol{\omega} \cdot \nabla)\boldsymbol{u},$$
$$\frac{D\boldsymbol{W}}{Dt} = (\boldsymbol{W} \cdot \nabla)\boldsymbol{u}.$$

Assume that they are related by a linear transformation $\boldsymbol{\mathcal{A}}$ at $t = 0$ such that

$$\boldsymbol{W}(0) = \boldsymbol{\mathcal{A}}(0)\boldsymbol{\omega}(0).$$

Then, for

$$\boldsymbol{W}(t) = \boldsymbol{\mathcal{A}}(t)\boldsymbol{\omega}(t) \quad (17)$$

to hold at any $t \geq 0$, it is necessary and sufficient that $\boldsymbol{\mathcal{A}}$ satisfies

$$\frac{D\boldsymbol{\mathcal{A}}}{Dt} = \boldsymbol{V}\boldsymbol{\mathcal{A}} - \boldsymbol{\mathcal{A}}\boldsymbol{V}, \quad (18)$$

where $\boldsymbol{V} = \nabla \boldsymbol{u}$ is the velocity gradient. (This is a variant, i.e. a 3D generalisation of an exercise given in [55].) The equation (18) can be solved as

$$\boldsymbol{\mathcal{A}}(t) = \boldsymbol{J(t)}\boldsymbol{\mathcal{A}}(0)\boldsymbol{J(t)}^{-1},$$

using the Jacobian matrix $J_{ij}(t) = \dfrac{\partial x_i}{\partial a_j};\ i, j = 1, 2, 3$, which obeys

$$\frac{D\boldsymbol{J}}{Dt} = \boldsymbol{V}\boldsymbol{J}.$$

Now, assume that a perfect alignment $\boldsymbol{\omega} \parallel \boldsymbol{W}$ is established between $\boldsymbol{\omega}$ and $\boldsymbol{W}$ at time $t = T$. Then by (17), the matrix $\boldsymbol{\mathcal{A}}$ is singular at that time, $\det(\boldsymbol{\mathcal{A}}(T)) = 0$. However,

$$\begin{aligned}\det(\boldsymbol{\mathcal{A}}(t)) &= \det(\boldsymbol{J(t)}\boldsymbol{\mathcal{A}}(0)\boldsymbol{J(t)}^{-1}) \\ &= \det(\boldsymbol{J(t)})\det(\boldsymbol{\mathcal{A}}(0))\det(\boldsymbol{J(t)}^{-1}) \\ &= \det(\boldsymbol{\mathcal{A}}(0)) \neq 0,\end{aligned}$$

so long as the flow remains smooth. We conclude by contradiction that the flow is not smooth at $t = T$.

It is clear that the same statement holds for two area element vectors, e.g. the impulse $\boldsymbol{\gamma}$ and a passive area element $\boldsymbol{A}$.

4. Differential geometric results

4.1. Fundamental equations

We consider the kinematics of vorticity surfaces in some detail. Using classical differential geometry, we describe the vorticity surface spanned by $\boldsymbol{x}_u = \boldsymbol{\omega}$ and $\boldsymbol{x}_v = \boldsymbol{W}$, whose unit normal vector is given by $\boldsymbol{e}$, $\boldsymbol{e} \equiv \boldsymbol{\gamma}/|\boldsymbol{\gamma}|$, see e.g. [68, 59]. Note that this can be written

$$\boldsymbol{e} = \frac{\boldsymbol{x}_u \times \boldsymbol{x}_v}{|\boldsymbol{x}_u \times \boldsymbol{x}_v|} = \frac{\boldsymbol{x}_u \times \boldsymbol{x}_v}{\sqrt{EG - F^2}} = \frac{\boldsymbol{\omega} \times \boldsymbol{W}}{|\boldsymbol{\omega} \times \boldsymbol{W}|},$$

where E, F and G denote the coefficients of first fundamental forms, respectively.

We recall that first, second and third fundamental forms are defined by

$$I \equiv \boldsymbol{dx} \cdot \boldsymbol{dx} = Edu^2 + 2Fdudv + Gdv^2,$$

$$II \equiv -\boldsymbol{dx} \cdot \boldsymbol{de} = Ldu^2 + 2Mdudv + Ndv^2$$

and

$$III \equiv \boldsymbol{de} \cdot \boldsymbol{de} = \widetilde{E}du^2 + 2\widetilde{F}dudv + \widetilde{G}dv^2,$$

where

$$E = \boldsymbol{x}_u \cdot \boldsymbol{x}_u = |\boldsymbol{\omega}|^2,\ F = \boldsymbol{x}_u \cdot \boldsymbol{x}_v = \boldsymbol{\omega} \cdot \boldsymbol{W},\ G = \boldsymbol{x}_v \cdot \boldsymbol{x}_v = |\boldsymbol{W}|^2,$$

$$L = \boldsymbol{x}_{uu} \cdot \boldsymbol{e} = \boldsymbol{\omega}_u \cdot \boldsymbol{e},\ M = \boldsymbol{x}_{uv} \cdot \boldsymbol{e} = \boldsymbol{\omega}_v \cdot \boldsymbol{e} (= \boldsymbol{W}_u \cdot \boldsymbol{e}),\ N = \boldsymbol{x}_{vv} \cdot \boldsymbol{e} = \boldsymbol{W}_v \cdot \boldsymbol{e},$$

and

$$\widetilde{E} = \boldsymbol{e}_u^2, \widetilde{F} = \boldsymbol{e}_u \cdot \boldsymbol{e}_v, \widetilde{G} = \boldsymbol{e}_v^2.$$

Note that $\widetilde{E}, \widetilde{F}$ and $\widetilde{G}$ represent the first fundamental form on the unit sphere.

For the surface $g = \text{const.}$, a set of equations for the surface called the Gauss-Weingarten equations, which corresponds to Frenet-Serre formulas for space curves, read ¶

$$\frac{\partial \boldsymbol{\omega}}{\partial u} = \Gamma^u_{uu}\boldsymbol{\omega} + \Gamma^v_{uu}\boldsymbol{W} + L\boldsymbol{e}, \tag{19}$$

¶ Note that $(\boldsymbol{\omega}, \boldsymbol{W}, \boldsymbol{e})$ does *not* form an orthogonal basis, as opposed to yet another representation of a surface by the so-called Darboux-Cartan moving frame. Here we use non-orthonormal basis as we need to handle the material vector $\boldsymbol{W}$, which is in general not orthogonal to $\boldsymbol{\omega}$.

$$\frac{\partial \boldsymbol{\omega}}{\partial v} = \Gamma^u_{uv}\boldsymbol{\omega} + \Gamma^v_{uv}\boldsymbol{W} + M\boldsymbol{e}, \tag{20}$$

$$\frac{\partial \boldsymbol{W}}{\partial u} = \Gamma^u_{vu}\boldsymbol{\omega} + \Gamma^v_{vu}\boldsymbol{W} + M\boldsymbol{e}, \tag{21}$$

$$\frac{\partial \boldsymbol{W}}{\partial v} = \Gamma^u_{vv}\boldsymbol{\omega} + \Gamma^v_{vv}\boldsymbol{W} + N\boldsymbol{e}, \tag{22}$$

$$\frac{\partial \boldsymbol{e}}{\partial u} = \frac{FM - GL}{EG - F^2}\boldsymbol{\omega} + \frac{FL - EM}{EG - F^2}\boldsymbol{W} \tag{23}$$

and

$$\frac{\partial \boldsymbol{e}}{\partial v} = \frac{FN - GM}{EG - F^2}\boldsymbol{\omega} + \frac{FM - EN}{EG - F^2}\boldsymbol{W}. \tag{24}$$

Note that equations (21) and (22) are equivalent. Here, Christoffel symbols are defined by

$$\Gamma^u_{uu} = \frac{GE_u - 2FF_u + FE_v}{2(EG - F^2)},\ \Gamma^u_{uv} = \frac{GE_v - FG_u}{2(EG - F^2)},\ \Gamma^u_{vv} = \frac{2GF_v - GG_u - FG_v}{2(EG - F^2)},$$

and

$$\Gamma^v_{uu} = \frac{2EF_u - EE_v - FE_u}{2(EG - F^2)},\ \Gamma^v_{uv} = \frac{EG_u - FE_v}{2(EG - F^2)},\ \Gamma^v_{vv} = \frac{EG_v - 2FF_v + FG_u}{2(EG - F^2)}.$$

In matrix notation, we can write

$$\frac{\partial}{\partial u}\begin{pmatrix} \boldsymbol{\omega} \\ \boldsymbol{W} \\ \boldsymbol{e} \end{pmatrix} = \begin{pmatrix} \Gamma^u_{uu} & \Gamma^v_{uu} & L \\ \Gamma^u_{vu} & \Gamma^v_{vu} & M \\ \dfrac{FM - GL}{EG - F^2} & \dfrac{FL - EM}{EG - F^2} & 0 \end{pmatrix}\begin{pmatrix} \boldsymbol{\omega} \\ \boldsymbol{W} \\ \boldsymbol{e} \end{pmatrix} \tag{25}$$

and

$$\frac{\partial}{\partial v}\begin{pmatrix} \boldsymbol{\omega} \\ \boldsymbol{W} \\ \boldsymbol{e} \end{pmatrix} = \begin{pmatrix} \Gamma^u_{uv} & \Gamma^v_{uv} & M \\ \Gamma^u_{vv} & \Gamma^v_{vv} & N \\ \dfrac{FN - GM}{EG - F^2} & \dfrac{FM - EN}{EG - F^2} & 0 \end{pmatrix}\begin{pmatrix} \boldsymbol{\omega} \\ \boldsymbol{W} \\ \boldsymbol{e} \end{pmatrix}. \tag{26}$$

This system of the Gauss-Weingarten equations are known to be over-complete; there are 15 scalar equations for 9 variables. Compatibility conditions yield the Coddazi-Mainardi equations and the Gauss equation (*Theorema Egregium* for the Gaussian curvature, **Appendix C**). The first 2 of the 6 compatibility conditions of Coddazi-Mainardi are

$$\frac{\partial L}{\partial v} - \frac{\partial M}{\partial u} = L\Gamma^u_{uv} + M(\Gamma^v_{uv} - \Gamma^u_{uu}) - N\Gamma^v_{uu} \tag{27}$$

and

$$\frac{\partial M}{\partial v} - \frac{\partial N}{\partial u} = L\Gamma^u_{vv} + M(\Gamma^v_{vv} - \Gamma^u_{uv}) - N\Gamma^v_{uv}. \tag{28}$$

4.2. Curvatures

We consider curvatures of the vorticity surface, see [68] for general descriptions. By the Weingarten equations (23,24), we have

$$\begin{aligned}\boldsymbol{e}_u \times \boldsymbol{e}_v &= \frac{(FM-GL)(FM-EN)-(FL-EM)(FN-GM)}{(EG-F^2)^2}\boldsymbol{x}_u \times \boldsymbol{x}_v \\ &= \frac{LN-M^2}{EG-F^2}\boldsymbol{x}_u \times \boldsymbol{x}_v \\ &= K\boldsymbol{x}_u \times \boldsymbol{x}_v.\end{aligned}$$

The normal curvature κ_n of the surface is defined by

$$\kappa_n = -\frac{\boldsymbol{dx}\cdot\boldsymbol{de}}{\boldsymbol{dx}\cdot\boldsymbol{dx}} = \frac{II}{I},$$

Associated with it, we have the Gaussian curvature K defined by

$$K = \kappa_1\kappa_2 = \frac{LN-M^2}{EG-F^2} = \frac{\boldsymbol{e}\cdot(\boldsymbol{e}_u\times\boldsymbol{e}_v)}{|\boldsymbol{\gamma}|} = \frac{1}{|\boldsymbol{\gamma}|^4}\left[(\boldsymbol{\omega}_u\cdot\boldsymbol{\gamma})(\boldsymbol{W}_v\cdot\boldsymbol{\gamma})-(\boldsymbol{\omega}_v\cdot\boldsymbol{\gamma})^2\right], \quad (29)$$

where κ_1 and κ_2 are principal curvatures. Note that $\boldsymbol{\omega}_v = \boldsymbol{W}_u$ by definition. Note also that the behaviour of K is subject to geometric depletion; that is, even if $|\boldsymbol{\gamma}| \to \infty$ it is ambiguous to see how K behaves from the expression (29). We will discuss its behaviour below. The mean curvature m is defined by

$$m = \frac{\kappa_1+\kappa_2}{2} = \frac{EN+GL-2FM}{2(EG-F^2)}.$$

There is an identity between the Gaussian curvature K, the mean curvature m and fundamental forms:

$$KI - 2mII + III = 0.$$

On the other hand, geodesic (that is, tangential) curvature is defined by [68]

$$\kappa_g = \boldsymbol{x}'(s)\cdot(\boldsymbol{x}''(s)\times\boldsymbol{e})$$

$$\begin{aligned}= \big[&\Gamma^v_{uu}u'(s)^3 + (2\Gamma^v_{uv}-\Gamma^u_{uu})u'(s)^2v'(s) + (\Gamma^v_{vv}-2\Gamma^u_{uv})u'(s)v'(s)^2 \\ &-\Gamma^u_{vv}v'(s)^3 + u'(s)v''(s) - u''(s)v'(s)\big]\sqrt{EG-F^2},\end{aligned}$$

where s denotes the arc length along the curve on the surface. It is a bending invariant, that is, determined solely in terms of the first fundamental form and its derivatives. We also recall that the vortex line is a geodesic on the surface if and only if $\boldsymbol{e}$ (the normal vector to the surface) and $\boldsymbol{n}$ (the normal vector of the vortex line) coincide. In that special case we have $\kappa_g = 0$ along the vortex line. In fact, we will see that something completely opposite happens if a singularity is to take place. To see this, we will derive a constraint showing the magnitude of K cannot become very large.

Recall the definition of the Gaussian curvature by spherical image, which states that

$$\begin{aligned}\Delta A_s \quad &= \sqrt{\widetilde{E}\widetilde{G} - \widetilde{F}^2}dudv, \\ \| \\ |K|\Delta A &= |K|\sqrt{EG - F^2}dudv,\end{aligned}$$

where ΔA and ΔA_s denote an area element on the surface and its spherical image, respectively. It follows that

$$K = \lim_{\Delta A \to 0} \frac{\Delta A_s}{\Delta A} = \frac{\sqrt{\widetilde{E}\widetilde{G} - \widetilde{F}^2}}{\sqrt{EG - F^2}}$$

with the appropriate sign. Actually, it is known that

$$|K|\sqrt{EG - F^2} = \sqrt{\widetilde{E}\widetilde{G} - \widetilde{F}^2}$$

holds generally [26, 29]. Because $|\boldsymbol{\gamma}| = \sqrt{EG - F^2}$, we have

$$|K||\boldsymbol{\gamma}| = \sqrt{\widetilde{E}\widetilde{G} - \widetilde{F}^2}.$$

Assume that we have a point-wise singularity in $|\boldsymbol{\gamma}|$ at $t = t_*$. Just before the breakdown $t = t_* - \epsilon$ ($\epsilon > 0$), we deduce a constraint on the Gaussian curvature

$$\int_D |K||\boldsymbol{\gamma}|dudv \leq 4\pi,$$

where D encloses the near-singular point. The integral can be made small by choosing D sufficiently small. In particular, the Gaussian curvature tends to vanish $K \to 0$ if the Jacobian associated with the Gauss's spherical image is bounded; $0 < \sqrt{\widetilde{E}\widetilde{G} - \widetilde{F}^2} < \infty$ at $t = t_*$ when $|\boldsymbol{\gamma}| \to \infty$.[+] In this case the singular point is a parabolic point. Hence if a singularity forms the vorticity surface locally looks like a plane $L = M = N = 0$, or a parabolic cylinder with $LN - M^2 = 0$ and $L^2 + M^2 + N^2 \neq 0$. If the Jacobian associated with the Gauss's spherical image becomes unbounded, we do not know how K behaves point-wise. For a number of expressions for $|K|$, see **Appendix D**.

4.3. Application of Gauss-Bonnet theorem

We have derived a constraint on the size of the Gaussian curvature K, which is related to the normal curvature. Here we ask what happens to the tangential curvature. By applying the Gauss-Bonnet theorem just before $t = t_*$ using a small closed circuit C around the singular point lying on the surface g =const, we find

$$\oint_C \kappa_g ds + \iint_D K dA = 2\pi.$$

[+] With the standard parametrisation (θ, ϕ) of the unit sphere we can write $\sqrt{\widetilde{E}\widetilde{G} - \widetilde{F}^2}dudv = \sin\theta d\theta d\phi$, Hence $\sqrt{\widetilde{E}\widetilde{G} - \widetilde{F}^2} = |\sin\theta| \left|\frac{\partial(\theta,\phi)}{\partial(u,v)}\right| \leq \left|\frac{\partial(\theta,\phi)}{\partial(u,v)}\right|$, which is bounded if $\frac{\partial(u,v)}{\partial(\theta,\phi)} \neq 0$.

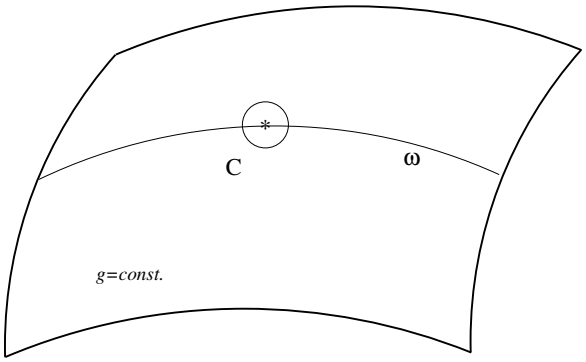

Figure 2. Application of the Gauss-Bonnet theorem to the vorticity surface. A closed circuit C encloses a near-singularity denoted by a star.

The second term $\iint_D K dA = \iint_{D'} dA_s$ on the left-hand side can be made $\neq 2\pi$, where D' is the spherical image of D. This term can be made as small as wish by choosing D sufficiently small and we have

$$\oint_C \kappa_g ds \approx 2\pi.$$

Because the arc length around C is also short, $|\kappa_g|$ must be very large in the neighborhood of the near-singularity. Recall that the geodesic curvature κ_g measures the curvature of a vortex line *lying* on the surface. This is consistent with previous works, which state that the curvature of a vortex line must behave wildly for a singularity to develop [19, 18].

5. Specific examples

5.1. Expressions for Clebsch potentials

So far we have been considering flows which have Clebsch potentials defined everywhere. This may be possible for flows in whole space, but not those under periodic boundary conditions. Indeed, some flows under periodic boundaries have Clebsch potentials with singularities; e.g. the Kida-Pelz flow and the Taylor-Green vortex. We will explore explicit formulas for them to identify an exceptional set of points where Clebsch potentials are absent.

It should be noted that the Taylor-Green vortex and the Kida-Pelz flow belong to the class of high-symmetric flows. Apparently, demanding even higher symmetry would trivialise the dynamics resulting in Beltrami types of steady flows, e.g. [8]. For general investigations on the Kida-Pelz flow, see[11, 12, 15].

The Taylor-Green vortex

The initial velocity field [70, 13] reads

$$\boldsymbol{u} = \begin{pmatrix} \sin x \cos y \cos z \\ \cos x \sin y \cos z \\ 0 \end{pmatrix}$$

and the following form of potentials have been found in [51]

$$\begin{cases} f = \sqrt{2} \cos x \sqrt{\cos z}, \\ g = \sqrt{2} \cos y \sqrt{\cos z}. \end{cases}$$

They have mild singularities at the boundary $z = \pi/2$, that is, they are continuous but not differentiable. See **Appendix B**.

The Kida-Pelz flow

The initial velocity and the vorticity fields in a box of $0 \le x, y, z \le \pi/2$ read

$$\boldsymbol{u} = \begin{pmatrix} \sin x(\cos 3y \cos z - \cos y \cos 3z) \\ \sin y(\cos 3z \cos x - \cos z \cos 3x) \\ \sin z(\cos 3x \cos y - \cos x \cos 3y) \end{pmatrix}$$

and

$$\boldsymbol{\omega} = \begin{pmatrix} -2 \cos 3x \sin y \sin z + 3 \cos x(\sin 3y \sin z + \sin y \sin 3z) \\ -2 \cos 3y \sin z \sin x + 3 \cos y(\sin 3z \sin x + \sin z \sin 3x) \\ -2 \cos 3z \sin x \sin y + 3 \cos z(\sin 3x \sin y + \sin x \sin 3y) \end{pmatrix}.$$

It can be checked, with the help of computer algebra, that the Frobenius condition holds

$$\boldsymbol{u} \cdot \boldsymbol{\omega} \equiv 0$$

and the Kida-Pelz flow has Clebsch potentials in some domain. Here we show two examples of the impulse variable $\boldsymbol{\gamma}$ which is not solenoidal. Their derivations and those of the solenoidal counterparts are given in **Appendices B** and **C**.

The first example of Clebsch potentials reads*

$$\begin{cases} f = 2\dfrac{(\cos x)^{3/2}(\cos^2 y - \cos^2 z)}{(\cos y \cos z)^{1/2}}, \\ g = 2\dfrac{(\cos y)^{3/2}(\cos^2 z - \cos^2 x)}{(\cos z \cos x)^{1/2}}, \\ h = 2\dfrac{(\cos z)^{3/2}(\cos^2 x - \cos^2 y)}{(\cos x \cos y)^{1/2}}, \end{cases}$$

where only two of them are independent. See **Appendix A** for the derivations. We can confirm that

$$\boldsymbol{\omega} = \nabla f \times \nabla g$$

* The denominator of f, $(\cos y \cos x)^{1/2}$ in [54], should read $(\cos y \cos z)^{1/2}$ as presented here.

holds. For this choice, the components of $\boldsymbol{\gamma} = f\nabla g$ are

$$\begin{cases} \gamma_1 = \dfrac{2\sin x\cos y(3\cos^2 x + \cos^2 z)(\cos^2 y - \cos^2 z)}{\cos z}, \\ \gamma_2 = \dfrac{6\cos x\sin y(\cos^2 x - \cos^2 z)(\cos^2 y - \cos^2 z)}{\cos z}, \\ \gamma_3 = \dfrac{-2\cos x\cos y\sin z(3\cos^2 z + \cos^2 x)(\cos^2 y - \cos^2 z)}{\cos^2 z}. \end{cases}$$

Note that $\nabla\cdot\boldsymbol{\gamma} \neq 0$. In fact, we need

$$\phi = 2\cos x\cos y\cos z(\cos^2 x + \cos^2 y - \cos^2 z) - \frac{2\cos^3 x\cos^3 y}{\cos z}$$

for a solenoidal projection $\boldsymbol{u} = \boldsymbol{\gamma} - \nabla\phi$.

The second example is

$$\begin{cases} \tilde{f} = \dfrac{\cos^2 y(\cos^2 z - \cos^2 x)}{\cos^2 z(\cos^2 y - \cos^2 x)}, \\ \tilde{g} = \dfrac{\cos^2 z(\cos^2 x - \cos^2 y)}{\cos^2 x(\cos^2 z - \cos^2 y)}, \\ \tilde{h} = \dfrac{\cos^2 x(\cos^2 y - \cos^2 z)}{\cos^2 y(\cos^2 x - \cos^2 z)}. \end{cases}$$

If we define by using the first example

$$h' = -2\frac{(\cos z)^3(\cos^2 x - \cos^2 y)^2}{\cos x\cos y},$$

then we have $\boldsymbol{\gamma} = \tilde{f}\nabla h' = \boldsymbol{u} + \nabla\phi$. The components of $\boldsymbol{\gamma}$ are

$$\begin{cases} \gamma_1 = \dfrac{2\sin x\cos y\cos z(3\cos^2 x + \cos^2 y)(\cos^2 x - \cos^2 z)}{\cos^2 x}, \\ \gamma_2 = -\dfrac{2\sin y\cos z(3\cos^2 y + \cos^2 x)(\cos^2 x - \cos^2 z)}{\cos x}, \\ \gamma_3 = -\dfrac{6\cos y\sin z(\cos^2 x - \cos^2 z)(\cos^2 y - \cos^2 x)}{\cos x}, \end{cases}$$

with

$$\phi = 2\cos x\cos y\cos z(\cos^2 y + \cos^2 z - \cos^2 x) - \frac{2\cos^3 y\cos^3 z}{\cos x}.$$

A comment may be in order. As already mentioned, the result of [35] states that near generic vorticity nulls, there are singularities in Clebsch potentials. It should be noted that its converse does not hold, that is, Clebsch potentials can have singularities near a point which is not a generic vorticity null. In fact, there are singular points which are not even vorticity nulls.

For example, consider the expression of the first kind. At $z = \pi/2$, clearly f does not exist. There we compute that

$$\begin{cases} \omega_1 = 4\cos x \sin y(-2\cos^2 x + 3\cos^2 y), \\ \omega_2 = 4\cos y \sin x(-2\cos^2 y + 3\cos^2 x), \\ \omega_3 = 0. \end{cases}$$

It is readily seen that on the plane $z = \pi/2$, $\boldsymbol{\omega} \neq 0$ except at $(x, y, z) = (0, 0, \pi/2), (\pi/2, \pi/2, \pi/2)$. This shows that the set of points where Clebsch potentials is unavailable are not restricted to vorticity nulls.

On the plane $z = \pi/2$, the velocity is

$$\begin{cases} u_1 = 0, \\ u_2 = 0, \\ u_3 = \cos 3x \cos y - \cos x \cos 3y, \end{cases}$$

and not all the points on the plane are stagnation points. The fluid particles initially on the plane start moving under the evolution of 3D Euler equations. Also, these singularities cannot be eliminated by canonical transformations; see the examples in **Appendix C**.

5.2. Exceptional set as separatrices

In the above examples, we have seen that the Clebsch potentials are not defined everywhere, but there are exceptional points at which they have singularities. It seems that the difficulty of having Clebsch potentials everywhere is regarded as a serious obstacle in their practical applications. Here, after characterising the nature of the singular sets, we propose to take advantage of their singularities to identify fluid particles associated with potential blowup.

Let us define a singular set of points Σ by

$$\Sigma = \{\boldsymbol{x} | f(x, y, z) \text{ or } g(x, y, z) \text{ is undefined or zero}\}$$

and consider the following decomposition of the whole space as follows

$$\mathbb{R}^3 = \Sigma \cup (\mathbb{R}^3 \setminus \Sigma).$$

In all the examples we came across, Σ is "thin" and they take the form of vorticity surfaces (sets of measure zero).

First, consider a snapshot of a smooth vorticity field at an instant of time. By definition, vortex lines starting from $\boldsymbol{x} \in \Sigma$ will remain there. Then vortex lines starting from $\boldsymbol{x} \in \mathbb{R}^3 \backslash \Sigma$ cannot enter Σ. Therefore the singular set Σ defines a set of separatrices.

Second, consider the dynamics of the 3D Euler equations. Under their time evolution, the Helmholtz theorem [37] state that vortex lines are material and they maintain their identity as such; fluid particles associated with vortex lines in Σ may move in physical $\boldsymbol{x}$-space, but they stay put in material $\boldsymbol{a}$-space.

Alternatively we may argue as follows. Because Clebsch potentials are material at points where they are defined

$$\frac{Df}{Dt} = \frac{Dg}{Dt} = 0$$

and the exceptional set of points of measure zero are also material, as a complement of sets of regular points. (Actually they are vorticity surfaces and hence inevitably material.) The separatrices are material; they keep comprising the same set of fluid particles.

We have seen in previous sections that flows with Clebsch potentials are subject to severe geometric constraints and given some arguments toward excluding type I blowup. Because such an argument cannot be applied to the exceptional set Σ, we are led to infer that if a singularity develops, it is most likely to be associated with Σ.

For the Kida-Pelz flow, the separatrices include at least

$$\Sigma = \left\{ \boldsymbol{x} \in [0, \pi/2]^3 \,|x = \pi/2, y = \pi/2, z = \pi/2, x = y, y = z, z = x \right\}$$

whereas for the Taylor-Green vortex

$$\Sigma = \left\{ \boldsymbol{x} \in [0, \pi/2]^3 \,|x = \pi/2, y = \pi/2, z = \pi/2 \right\},$$

see **Appendix C**. We propose to use Σ as an indicator to locale possible singularity formation. It may be of interest to examine how the vorticity surfaces Σ evolve in time by numerical experiments.

6. Summary and outlook

A basic formulation of the 3D Euler equations based on Clebsch potentials is presented. We have studied how Clebsch potentials impose severe constraints on the vortex stretching mechanism in 3D Euler flows.

One result have come from the simple formula

$$\boldsymbol{W} \cdot \nabla f = f,$$

when when the right-hand side is not a null $f \neq 0$. This enforces $\boldsymbol{W}$ to be perpendicular to ∇f, triggering one of the geometric depletions $\boldsymbol{\omega} = \nabla f \times \nabla g$ or $\boldsymbol{\gamma} = \boldsymbol{\omega} \times \boldsymbol{W}$ coming into play. Strictly speaking, even for type I singularity blowup has not yet been ruled out completely, but we have argued that it is unlikely.

A simple analysis based on classical differential geometry of surfaces we have obtained the expression

$$|K||\boldsymbol{\gamma}| = \sqrt{\widetilde{E}\widetilde{G} - \widetilde{F}^2},$$

where the right-hand side is the Jacobian associated with the spherical image. An immediate consequence is that the curvature tends to vanish upon singularity if the Jacobian is bounded. This also impose a constraint on the size of the Gauss curvature

of the vortex surface. The Gauss-Bonnet theorem in turn shows that it is the tangential curvature that must go wild upon singularity.

Specific examples of Clebsch potentials are presented using initial conditions of high-symmetric flows. They show that there are exceptional sets of points (of measure zero) which can be regarded as separatrices. We have seen above that in some domain where Clebsch potentials are well-defined singularities are unlikely to show up. We thus infer if singularities develop they are likely to be located in the neighborhood of separatrices.

A few remarks may be in order on a related formulation. The equation for the vortex line parameterised by u is given by

$$\frac{d\boldsymbol{x}}{du} = \boldsymbol{\omega}(\boldsymbol{x}(u)) = \nabla f \times \nabla g.$$

For arbitrary function $F(\boldsymbol{x})$ defined along the vortex line, we have more generally

$$\frac{dF(\boldsymbol{x})}{du} = \boldsymbol{\omega} \cdot \nabla F = (\nabla f \times \nabla g) \cdot \nabla F = \frac{\partial(F, f, g)}{\partial(x, y, z)}$$

This is known as Nambu's generalised Hamiltonian form [49, 50]. In particular, taking $F = \phi$, we recover

$$\frac{\partial \phi}{\partial u} = \frac{\partial(\phi, f, g)}{\partial(x, y, z)} = -\boldsymbol{u} \cdot \boldsymbol{\omega}.$$

It may be of interest to combine such a formulation with the differential geometric approach outlined here.

It is of interest to tracing the Clebsch potentials in time e.g. in the Kida-Pelz flow by numerical simulations. Of particular interest is to check how the material separatrices behave in connection with possible singularity or near-singularity.

Appendix A. Elementary theorems in vectorial analysis [2, 64]

Theorem 1 If $\nabla \cdot \boldsymbol{a} = 0$, then there exists a vector $\boldsymbol{A}$ such that

$$\boldsymbol{a} = \nabla \times \boldsymbol{A},$$

or, alternatively there exist scalars λ and μ such that

$$\boldsymbol{a} = \nabla \times (\lambda \nabla \mu).$$

In this case, we can write $\boldsymbol{A} = \lambda \nabla \mu - \nabla \phi$ with some scalar ϕ.

For our purpose, we take $\boldsymbol{a} = \boldsymbol{\omega}$.

Theorem 2 If $\boldsymbol{a} \cdot (\nabla \times \boldsymbol{a}) \equiv 0$, there exist scalars λ and ϕ such that

$$\boldsymbol{a} = \lambda \nabla \phi.$$

For our purpose, we take $\boldsymbol{a} = \boldsymbol{\gamma}$.

It should be noted that standard proofs, e.g. those found in [2, 64], make use of an expression $\mu \boldsymbol{a} = \nabla\phi$, which assumes tacitly that $\lambda \neq 0$. In our context in (5), the statement can (and does) break down in the neighborhood of a null point of $f = 0$. This explains, at least partially, why the singular sets of Clebsch potentials have not been given proper attention so far.

Appendix B. Derivations of Clebsch potentials for the Kida-Pelz flow

We consider the Kida-Pelz flow in $0 \leq x, y, z \leq \pi/2$.

The equations for vortex lines

$$\frac{dx}{\omega_1} = \frac{dy}{\omega_2} = \frac{dz}{\omega_3}$$

take the following form

$$\frac{\tan x\, dx}{2\cos^2 x - 3\cos^2 y - 3\cos^2 z} = \frac{\tan y\, dy}{2\cos^2 y - 3\cos^2 z - 3\cos^2 x}$$

$$= \frac{\tan z\, dz}{2\cos^2 z - 3\cos^2 x - 3\cos^2 y}.$$

By introducing new variables

$$\xi = \cos^2 x,\ \eta = \cos^2 y,\ \zeta = \cos^2 z$$

we may write

$$\frac{d\xi}{\xi\,(2\xi - 3(\eta+\zeta))} = \frac{d\eta}{\eta\,(2\eta - 3(\zeta+\xi))} = \frac{d\zeta}{\zeta\,(2\zeta - 3(\xi+\eta))},$$

or

$$\frac{d\eta}{d\xi} = \frac{\eta\,(2\eta - 3(\zeta+\xi))}{\xi\,(2\xi - 3(\eta+\zeta))},\ \frac{d\zeta}{d\xi} = \frac{\zeta\,(2\zeta - 3(\xi+\eta))}{\xi\,(2\xi - 3(\eta+\zeta))}.$$

By setting $Y = \eta/\xi,\ Z = \zeta/\xi$, we have

$$\xi\frac{dY}{d\xi} = \frac{5Y(Y-1)}{2-3(Y+Z)}, \tag{B.1}$$

$$\xi\frac{dZ}{d\xi} = \frac{5Z(Z-1)}{2-3(Y+Z)}. \tag{B.2}$$

From these we find

$$\frac{dZ}{dY} = \frac{Z(Z-1)}{Y(Y-1)}$$

which is integrated to give a first integral

$$\frac{Z-1}{Z}\frac{Y}{Y-1} = C,$$

or

$$\frac{\cos^2 y}{\cos^2 z}\,\frac{\cos^2 z-\cos^2 x}{\cos^2 y-\cos^2 x}=C. \tag{B.3}$$

Substituting $Z=\dfrac{Y}{(1-C)Y+C}$ into (B.2), we find

$$\frac{d\xi}{\xi}=\frac{1}{5}\frac{3(1-C)Y^2+(1+5C)Y+2C}{Y(Y-1)(C-1)Y-C}dY.$$

Integrating, we get

$$\log|\xi|=-\frac{2}{5}\log|Y|-\frac{4}{5}\log|Y-1|+\frac{3}{5}\log|-Y+YC-C|+C',$$

or

$$\xi=C''\frac{|(C-1)Y-C|^{3/5}}{Y^{2/5}(Y-1)^{4/5}}=C''\frac{|\frac{Y}{Z}|^{3/5}}{Y^{2/5}(Y-1)^{4/5}},$$

where $C''=e^{C'}$. It follows that

$$\frac{(\eta-\xi)^4\zeta^3}{\xi\eta}=C'',$$

that is,

$$\frac{(\cos z)^6(\cos^2 x-\cos^2 y)^4}{(\cos x\cos y)^2}=C'. \tag{B.4}$$

Similarly, we obtain two other integrals.

We make use of (B.4) for the first example. We set tentatively

$$\begin{cases} f=\dfrac{(\cos x)^3(\cos^2 y-\cos^2 z)^2}{\cos y\cos z},\\ g=\dfrac{(\cos y)^3(\cos^2 z-\cos^2 x)^2}{\cos z\cos x},\\ h=\dfrac{(\cos z)^3(\cos^2 x-\cos^2 y)^2}{\cos x\cos y} \end{cases}$$

and we consider

$$\nabla f^n\times\nabla g^n=n^2(fg)^{n-1}\nabla f\times\nabla g,$$

because if f is material, so is f^n. By demanding that

$$\frac{|\boldsymbol{\omega}|}{(fg)^{n-1}|\nabla f\times\nabla g|}=\text{const},$$

we find $n=1/2$ and const $=1$. By redefining $2f^{1/2}\to f$ and $2g^{1/2}\to g$, we obtain the first example.

Making use of (B.3), we set for the second example

$$\begin{cases} \tilde{f} = \dfrac{\cos^2 y(\cos^2 z - \cos^2 x)}{\cos^2 z(\cos^2 y - \cos^2 x)}, \\ \tilde{g} = \dfrac{\cos^2 z(\cos^2 x - \cos^2 y)}{\cos^2 x(\cos^2 z - \cos^2 y)}, \\ \tilde{h} = \dfrac{\cos^2 x(\cos^2 y - \cos^2 z)}{\cos^2 y(\cos^2 x - \cos^2 z)}. \end{cases}$$

It can be checked that they are not independent, that is, $\nabla\tilde{f} \times \nabla\tilde{g} \equiv 0$ etc. but if the first example is used, we have e.g. $\nabla\tilde{f} \times \nabla h = -\frac{1}{2}\boldsymbol{\omega}$. By defining

$$h' = -2\frac{(\cos z)^3(\cos^2 x - \cos^2 y)^2}{\cos x \cos y},$$

we can write

$$\boldsymbol{\omega} = \nabla\tilde{f} \times \nabla h'.$$

Appendix C. Canonical transformations

We present solenoidal counterparts of $\boldsymbol{\gamma}$, i.e. the incompressible velocity $\boldsymbol{u}$ based on an application of canonical transformations. We keep writing f, g, ϕ to denote non-solenoidal potentials described above and consider

$$f = \frac{\partial S}{\partial g},\ F = -\frac{\partial S}{\partial G} \text{ with } \Phi = \phi - S(g, G),$$

to generate new potentials

$$\boldsymbol{u} = F\nabla G - \nabla\Phi = f\nabla g - \nabla\phi.$$

As noted in Section 1, all the Clebsch potentials related by canonical transformations are equivalent. Singular points and nulls observed in a particular choice of potentials cannot be eliminated by such a transformation. Hence the separatrices $\boldsymbol{\Sigma}$ include the union of singularities of f or g, and zeros of f or g.

The Taylor-Green vortex

The original non-solenoidal potentials are

$$\begin{cases} f = \sqrt{2}\cos x\sqrt{\cos z}, \\ g = \sqrt{2}\cos y\sqrt{\cos z}, \\ \phi = \cos x \cos y \cos z (= fg/2). \end{cases}$$

The expressions f and g were given by [51], whereas the form of Φ is determined by $\nabla \cdot \boldsymbol{u} = 0$. By choosing a generating function

$$S(g, G) = \frac{g^2}{2G},$$

we find

$$\begin{cases} F = \cos^2 x \cos z, \\ G = \dfrac{\cos y}{\cos x}, \\ \Phi = 0. \end{cases}$$

The exceptional set for the Taylor-Green vortex is obtained as a union of singularities and zeros of f, g, F and G.

$$\Sigma = \left\{ \boldsymbol{x} \,\middle|\, x = \frac{\pi}{2}, y = \frac{\pi}{2}, z = \frac{\pi}{2} \right\},$$

that is, separatrices include those points.

The Kida-Pelz flow: example 1

The original choice is

$$\begin{cases} f = 2\dfrac{(\cos x)^{3/2}(\cos^2 y - \cos^2 z)}{(\cos y \cos z)^{1/2}}, \\ g = 2\dfrac{(\cos y)^{3/2}(\cos^2 z - \cos^2 x)}{(\cos z \cos x)^{1/2}}, \\ \phi = 2\cos x \cos y \cos z(\cos^2 x + \cos^2 y - \cos^2 z) - \dfrac{2\cos^3 x \cos^3 y}{\cos z} \left(= \frac{1}{2} fg\right) \end{cases}$$

By choosing

$$S(g, G) = -\frac{g^2}{2G},$$

we find

$$\begin{cases} F = -2\dfrac{(\cos x)^3(\cos^2 y - \cos^2 z)^2}{\cos y \cos z}, \\ G = \dfrac{\cos^2 y(\cos^2 x - \cos^2 z)}{\cos^2 x(\cos^2 y - \cos^2 z)}, \\ \Phi = 0. \end{cases}$$

The Kida-Pelz flow: example 2

The original choice is

$$\begin{cases} f = \dfrac{\cos^2 y(\cos^2 z - \cos^2 x)}{\cos^2 z(\cos^2 y - \cos^2 x)}, \\ g = -2\dfrac{(\cos z)^3(\cos^2 x - \cos^2 y)^2}{\cos x \cos y}, \\ \phi = 2\cos x \cos y \cos z(\cos^2 y + \cos^2 z - \cos^2 x) - \dfrac{2\cos^3 y \cos^3 z}{\cos x} \, (= fg.) \end{cases}$$

By choosing

$$S(g, G) = \frac{g}{G},$$

we find

$$\begin{cases} F = -2\dfrac{(\cos y)^3(\cos^2 z - \cos^2 x)^2}{\cos z \cos x}, \\ G = \dfrac{\cos^2 z(\cos^2 y - \cos^2 x)}{\cos^2 y(\cos^2 z - \cos^2 x)}, \\ \Phi = 0. \end{cases}$$

The exceptional set for the Kida-Pelz flow is

$$\Sigma = \left\{ \boldsymbol{x} \,\middle|\, x = \frac{\pi}{2}, y = \frac{\pi}{2}, z = \frac{\pi}{2}, x = y, y = z, z = x \right\},$$

that is, separatrices include those points.

Appendix D. *Gauss's Theorema Egregium*

The Jacobian associated with Gauss's spherical image is given by $\sqrt{\widetilde{E}\widetilde{G} - \widetilde{F}^2} = H|K|$, where $H \equiv \sqrt{EG - F^2}$. *Theorema Egregium* allows explicit formulas for K. Gauss's original expression is lengthy [30]:

$$4H^4K = E\left[\frac{\partial E}{\partial v}\frac{\partial G}{\partial v} - 2\frac{\partial F}{\partial u}\frac{\partial G}{\partial v} + \left(\frac{\partial G}{\partial u}\right)^2\right] + F\left[\frac{\partial E}{\partial u}\frac{\partial G}{\partial v} - \frac{\partial E}{\partial v}\frac{\partial G}{\partial u} - 2\frac{\partial E}{\partial v}\frac{\partial F}{\partial v} - 2\frac{\partial F}{\partial u}\frac{\partial G}{\partial u} + 4\frac{\partial F}{\partial u}\frac{\partial F}{\partial v}\right]$$

$$+G\left[\frac{\partial E}{\partial u}\frac{\partial G}{\partial u} - 2\frac{\partial E}{\partial u}\frac{\partial F}{\partial v} + \left(\frac{\partial E}{\partial v}\right)^2\right] - 2H^2\left[\frac{\partial^2 E}{\partial v^2} - 2\frac{\partial^2 F}{\partial u \partial v} + \frac{\partial^2 G}{\partial u^2}\right].$$

There are a number of alternative forms, such as Liouville's [68]

$$K = \frac{1}{H}\left[\frac{\partial}{\partial v}\left(\frac{H}{E}\Gamma^v_{uu}\right) - \frac{\partial}{\partial u}\left(\frac{H}{E}\Gamma^v_{uv}\right)\right] = \frac{1}{H}\left[\frac{\partial}{\partial u}\left(\frac{H}{E}\Gamma^u_{vv}\right) - \frac{\partial}{\partial v}\left(\frac{H}{E}\Gamma^u_{uv}\right)\right],$$

its variant [67]

$$K = \frac{1}{2H}\left[\frac{\partial}{\partial u}\left(\frac{FE_v - EG_u}{EH}\right) + \frac{\partial}{\partial u}\left(\frac{2EF_u - FE_u - EE_v}{EH}\right)\right],$$

and Frobenius's [68]

$$K = -\frac{1}{H^4}\begin{vmatrix} E & F & G \\ E_u & F_u & G_u \\ E_v & F_v & G_v \end{vmatrix} - \frac{1}{2H}\left[\frac{\partial}{\partial u}\left(\frac{G_u - F_v}{H}\right) - \frac{\partial}{\partial v}\left(\frac{F_u - E_v}{H}\right)\right].$$

Acknowledgments

This work has been partially supported by an EPSRC grant: EP/N022548/1.

References

[1] Appell, P. *Tome triosiéme: équilibre et mouvement des milieus continus, in "Traité Mécanique Rationnelle* Gauthier-Villars, 1909, Paris.

[2] Aris, R. *Vectors, tensors, and the basic equations of fluid mechanics* Prentice-Hall, 1962, New York.

[3] Ashurst, W. T., Kerstein, A. R., Kerr, R. M., and Gibson, C. H. Alignment of vorticity and scalar gradient with strain rate in simulated NavierStokes turbulence *Phys. Fluids* **30**, 2343–2353.

[4] Bateman, H. 1929 Notes on a Differential Equation Which Occurs in the Two-Dimensional Motion of a Compressible Fluid and the Associated Variational Problems. *Proc. Roy. Soc. of London A* **125**, 598–618.

[5] Beale, J.T. , Kato, T. & Majda, A. 1984 Remarks on the breakdown of smooth solutions for the 3D Euler equations. *Commun. Math. Phys.* **94**, 61–66.

[6] Benjamin, T.B. 1984 Impulse, flow force and variational principles. *IMA J. Appl. Math.* **32**, 3–68.

[7] Bennett, A. 2006 Lagrangian Fluid Dynamics Cambridge University Press, Cambridge.

[8] Bogoyavlenskij, O. & Fuchssteiner, B. 2005 Exact NSE solutions with crystallographic symmetries and no transfer of energy through the spectrum. *Journal of Geometry and Physics* **54**, 324–338.

[9] Bohm, D. 1952 A Suggested Interpretation of the Quantum Theory in Terms of "Hidden" Variables. *Phys. Rev.* **85**, 166–179.

[10] Born, M. *Natural Philosophy of Cause and Chance* M. Born, Oxford at the Clarendon Press, 1951, Oxford

[11] Boratav, O. N. & Pelz, R. B. 1994 Direct numerical simulation of transition to turbulence from a high-symmetry initial condition. *Phys. Fluids* **6**, 2757–2784.

[12] Boratav, O.N. & Pelz, R.B. 1995 Locally isotropic pressure Hessian in a high-symmetry flow. *Phys. Fluids* **7**, 895–897.

[13] Brachet, M. E., Meiron, D. I., Orszag, S. A., Nickel, B. G., Morf R. H. & Frisch, U. 1983 Small-scale structure of the Taylor-Green vortex. *J. Fluid Mech.* **130**, 411–452.

[14] Bridges, T.J., Hydon, P.E. & Reich, S. 2005 Vorticity and symplecticity in Lagrangian fluid dynamics. *J. Phys. A: Math. and Gen.* **38**, 1403–1418.

[15] Cichowlas, C. & Brachet, M.-E. 2005 Evolution of complex singularities in Kida-Pelz and Taylor-Green inviscid flows. *Fluid Dyn. Res.* **36**, 239–248.

[16] Clebsch, A. 1857 Uber eine allgemeine Transformation der hydrodynamischen Gleichungen. *J. Reine Angew. Math.* **54**, 293–313 (in German).

[17] Clebsch, A. 1859 Uber die Integration der hydrodynamischen Gleichungen. *J. Reine Angew. Math.* **56**, 1–10 (in German).

[18] Constantin, P., Fefferman, Ch. & Majda, A. 1996 Geometric constraints on potentially singular solutions for the 3-D Euler equations. *Commun. Part. Diff. Eqn.* **21**, 559–571.

[19] Constantin, P. 1994 Geometric statistics in turbulence. *SIAM Review* **36**, 73–98.

[20] Constantin, P. 2001 An Eulerian-Lagrangian Approach for incompressible fluids: local theory. *J. Amer. Math. Soc.* **14**, 263–278.

[21] Cotter, C.J. & Holm, D.D. 2009 Continuous and discrete Clebsch variational principles. *Found. Comp. Math.* **9**, 221–242.

[22] Davydov, B. 1949 Variational principle and canonical equations for an ideal fluid. *Dokl. Akad. Nauk SSSR* **2**, 165–168.

[23] Deng, J., Hou, T.Y. & Yu, X. 2005 Geometric properties and non-blowup of 3-D incompressible Euler flow. *Commun. Part. Diff. Eqn.* **30**, 225–243.

[24] Duhem, P. 1901 Sur les équations de h'hydrodynamique. Commentaire a un mémoire de Clebsch. *Ann. Fac. Sci. Univ. Toulouse.* **3**, 253–279 (in French).

[25] Eckart, C. 1960 Variation Principles of Hydrodynamics. *Phys. of Fluids* **3**, 421–427.

[26] Eisenhart, L.P. *A Treatise on the Differential Geometry of Curves and Surfaces.* Ginn and Company, Bonston, 1909.
[27] Falkovich, G. & L'vov, V.S. 1995 Isotropic and anisotropic turbulence in Clebsch variables. *Chaos, Solitons and Fractals* **5**, 1855–1869.
[28] Flanders, H. *Differential Forms with Applications to the Physical Science* Academic Press, 1963, New York.
[29] Forsyth, A.R. *Lectures on the differential geometry of curves and surfaces* Cambridge University Press, Cambridge, 1920.
[30] Gauss, K.F. *General Investigations of Curved Surfaces* Dover, New York, 2013.
[31] Gaffet, B. 1985 On generalized vorticity-conservation laws. *J. Fluid Mech.* **156**, 141–149.
[32] Galanti, B., Gibbon, J.D., & Heritage, M. 1997 Vorticity alignment results for the three-dimensional Euler and Navier-Stokes equations. *Nonlinearity* **10**, 1675.
[33] Gibbon, J.D. & Holm, D.D. 2010 The dynamics of the gradient of potential vorticity. *J. Phys. A: Math. Theor.* **43**, 172001.
[34] Gibbon, J.D. & Titi, E.S 2013 *The 3D incompressible Euler equations with a passive scalar: a road to blow-up?* J. Nonlinear Sci. **23**, 993 – 1000.
[35] Graham, C.R & Henyey, F.S. 2000 Clebsch representation near points where the vorticity vanishes. *Phys. Fluids* **12**, 744–746.
[36] Hadamard, J. 1949 *Lecons sur la propagation des ondes et les equations de l'hydrodynamique,* AMS Chelsea, 1949, New York.
[37] Helmholtz, H. 1858 Uber integrale der hydrodynamischen Gleichungen, welche den wirbelbewegungen entsprechen. *J. Reine Angew. Math.* **55**, 25–55 (in German).
[38] Hicks, W.M. 1881 Report on Recent Progress in Hydrodynamics PartI. *Rep. Brit. Ass. Advmt. Sci.* **51**, 57–88.
[39] Holm, D.D. & Kerr, R.M. 2007 Helicity in the formation of turbulence. *Phys. Fluids* **19**, 025101–9.
[40] Holm, D.D. & Kupershmidt, B.A. 1983 Poisson brackets and Clebsch representations for magnetohydrodynamics, multifluid plasmas, and elasticity. *Physica D* **6**, 347–363.
[41] Holm, D.D. & Kimura, Y. 1991 Zero-helicity Lagrangian kinematics of three-dimensional advection. *Phys. Fluids A* **3**, 1033–1038.
[42] Kambe, T. 2007 Gauge principle and variational formulation for ideal fluids with reference to translational symmetry. *Fluid Dyn. Res.* **39**, 98–120.
[43] Khalatnikov, I.M. 1952 The hydrodynamics of solutions of impurities in helium II. (in Russian) *Zh. Eksperim. i Teor. Fiz.* **23**, 169
[44] Khalatnikov, I.M. *An introduction to the theory of superfluidity,* translated by P.C. Hohenberg Benjamin, New York, Amsterdam, 1965.
[45] Kuznetsov, E.A. 2008 Mixed Lagrangian-Eulerian description of vortical flows for ideal and viscous fluids. *J. Fluid Mech.* **600**,167–180.
[46] Lin, C.C. 1987 Hydrodynamics of Helium II. in *Selected Papers of C.C. Lin with Commentary*, p.429, (ed.) D.J. Benney, F.H. Shu and C. Yuan, World Scientific, Singapore, 1987.
[47] Marsden, J.E. & Weinstein, A. 1983 Coadjoint orbits, vortices, and Clebsch variables for incompressible fluids. *Physica D* **7**, 305–323.
[48] Maslov, V.P. 1965 *Asymptotic methods and the theory of perturbations* Nauka. (in Russian).
[49] Nambu, Y. 1973 Generalized Hamiltonian Dynamics. *Phys. Rev. D* **7**, 2405–2412.
[50] Nevir, P. & Blender, R. 1993 A Nambu representation of incompressible hydrodynamics using helicity and enstrophy. *J. Phys. A: Math. Gen.* **26**, L1189–L1193.
[51] Nore, C., Abid, M. & Brachet, M. E. 1997 Decaying Kolmogorov turbulence in a model of superflow. *Phys. of Fluids* **9**, 2644–2669.
[52] Ohkitani, K. and Kishiba, S. 1995 Nonlocal nature of vortex stretching in an inviscid fluid. *Physics of Fluids* **7**, 411-421.
[53] Ohkitani, K. 1993 Eigenvalue problems in threedimensional Euler flows. *Physics of Fluids A* **5**,

2570-2572.

[54] Ohkitani, K. 2008 A Geometrical Study of 3D Incompressible Euler Flows with Clebsch potentials. *Physica D* **237**, 2020–2027.

[55] Ockendon, J., Howison, S., Lacey, A. and Movchan, A. 1999 *Applied partial differential equations.* Oxford University Press, Oxford.

[56] Ottino, J.M. 1989 *The kinematics of mixing : stretching, chaos, and transport.* Cambridge University Press, Cambridge.

[57] Panton, R.L. 1978 Potential/complex-lamellar velocity decomposition and its relevance to turbulence. *J. Fluid Mech.* **88**, 97–114.

[58] Roberts, M.D. The clebsch momenta approach to fluid lagrangians. arXiv:0910.3587v1 [gr-qc]

[59] Rogers, C. & Schief, W.K. 2002 *Backlund and Darboux Transformations: Geometry and Modern Applications in Soliton Theory.* Cambridge University Press.

[60] Rund, H. 1977 Clebsch potentials and variational principles in the theory of dynamical systems. *Arch. Rat. Mech. Anal.* **65**, 305–334.

[61] Russo, G. & Smereka, P. 1999 Impulse formulation of the Euler equations: General properties and numerical methods. *J. Fluid Mech.* **391**, 189–209.

[62] Rylov, Y.A. 2004 Hydrodynamic equations for incompressible inviscid fluid in terms of generalized stream function. *Int. J. Math. and Mat. Sci.* **11**, 541–570.

[63] Salmon, R. 1998 *Lectures on Geophysical Fluid Dynamics* Oxford University Press.

[64] Segel, L.A. *Mathematics Applied to Continuum Mechanics* L.A. Segel, Dover Publications, 1977, New York

[65] Seliger, R.L. & Whitham, G.B. 1968 Variational Principles in Continuum Mechanics. *Proc. Roy. Soc. Lond A* **305**, 1–25.

[66] Serrin, J. 1959 Mathematical Principles of Classical Fluid Mechanics. *in: S. Flügge & C. Truesdell (Eds.), Handbuch der Physik, Springer, Berlin*, 125–163.

[67] Stoker, J.J. *Differential Geometry.* John Wiley and Sons, New York, 1989.

[68] Struik, D.J. *Lectures on Classical Differential Geometry.* Dover, New York, 1988.

[69] Sudarshan, E.C.G. & Mukunda, N. *Classical Dynamics: A Modern Perspective* John Wiley & Sons, New York, 1974.

[70] Taylor, G. I. & Green, A. E. 1937 Mechanism of the production of small eddies from large ones. *Proc. Roy. Soc. London* A **158**, 499–521.

[71] Thomson, W. 1851 A Mathematical Theory of Magnetism *Phil. Trans. Roy. Soc.* **141**, 243–268, 269-285. Also, in "Reprint of papers on electrostatics and magnetism" 1872, Macmillan, London

[72] Truesdell, C. & Toupin, R.A. The classical field theories. in Handbuch der Physik III/1, 226 – 858, Springer, Berlin, 1960 ed. by S. Flügge.

[73] Truesdell, C. *The Kinematics of Vorticity.* Indiana University Press, 1954.

[74] Yokota, J.W. 1997 Potential/complex-lamellar descriptions of incompressible viscous flow. *Phys. Fluids* **9**, 2264–2272.

[75] Yoshida, Z. 2009 Clebsch parameterization: basic properties and remarks on its applications. *J. Math. Phys.* **50**, 113101–16.

[76] Zakharov, V.E. 1989 The algebra of integrals of motion of two-dimensional hydrodynamics in Clebsch variables *Functional Analysis and Its Applications* **23**, 24–31.